

# Analysis and interpretation of refractory microstructures in studies of corrosion mechanisms by liquid oxides

J. Poirier<sup>a,\*</sup>, F. Qafssaoui<sup>b</sup>, J.P. Ildefonse<sup>c</sup>, M.L. Bouchetou<sup>a</sup>

<sup>a</sup> CRMHT, 1D, avenue de la Recherche Scientifique 45071 Orléans cedex 2, France

<sup>b</sup> Moulay Ismaïl University, Faculty of Science, B.P. 4010 Zitoune, 50000 Meknes, Morocco

<sup>c</sup> Polytech'Orléans, 8 rue Léonard de Vinci, 45072 Orléans cedex 2, France

Received 1 August 2007; received in revised form 29 September 2007; accepted 7 October 2007

Available online 4 January 2008

## Abstract

The refractories must not only resist high temperatures but also corrosion by liquid oxides. This corrosion involves phenomena of dissolution and precipitation of new crystalline phases. The study of the microstructures of corroded refractories provides essential information. However, the interpretation of the microscopic observations is difficult. Indeed, because of the crystallization of liquid glasses during cooling, the mineral phases observed at room temperature are not representative of those observed at high temperature. The concept of local thermodynamic equilibrium and the use of the phase rule makes it possible to interpret the microstructures of corroded refractories, to explain the observed mineral zonation and to quantify the composition of the liquid phase at high temperature from chemical profiles established by SEM. Experimental data from corrosion of high alumina refractories will illustrate and validate this theoretical approach.

© 2007 Elsevier Ltd. All rights reserved.

**Keywords:** Refractories; Corrosion; Microstructure; Thermodynamic equilibrium; Electron microscopy

## 1. Introduction

The refractories are ceramics used to line many industrial high temperature furnaces. These materials are subjected to complex degradations such as thermal shock, erosion or chemical corrosion which can occur separately or together.

Corrosion by liquid oxides is one of the most severe modes of degradations which limit the lifetime of the refractory linings.

The examination of the microstructures<sup>1</sup> of refractories after use is extremely useful to evaluate the corrosion resistance of various refractories and to determine the mechanisms of chemical attack thus making it possible to propose new ways of improvements for the formulation of refractories.

However, the microstructures of corroded refractories are very difficult to interpret. The reasons are as follows:

- The refractories are multi-component and heterogeneous ceramics. Consequently, they have complex microstructures.

- The microscopic observations and the analyses are carried out at room temperature. They are not representative of the mineral and vitreous phases existing at high temperature.
- During cooling, new solid phases appear by crystallization of liquid oxides. The composition of the vitreous phases also evolves with the temperature (see Fig. 1).

Consequently, the information obtained is often limited and gives already known conclusions.

In this paper, we will present a method to analyse and interpret the microstructures of refractories after use. Typical examples of corrosion of high alumina-based refractories will be presented.

The experimental results, which are not well explained, will be re-analysed and clarified.

By using thermodynamic data and phase diagrams, the study of the microstructures will enable us to deduce:

- The proportion and the composition of the high temperature intergranular liquid phase.
- The gradients of the chemical properties between the hot face and the back of the refractory lining: the chemical profile of

\* Corresponding author. Tel.: +33 2 38 25 55 14; fax: +33 2 38 63 81 03.  
E-mail address: [Jacques.Poirier@univ-orleans.fr](mailto:Jacques.Poirier@univ-orleans.fr) (J. Poirier).

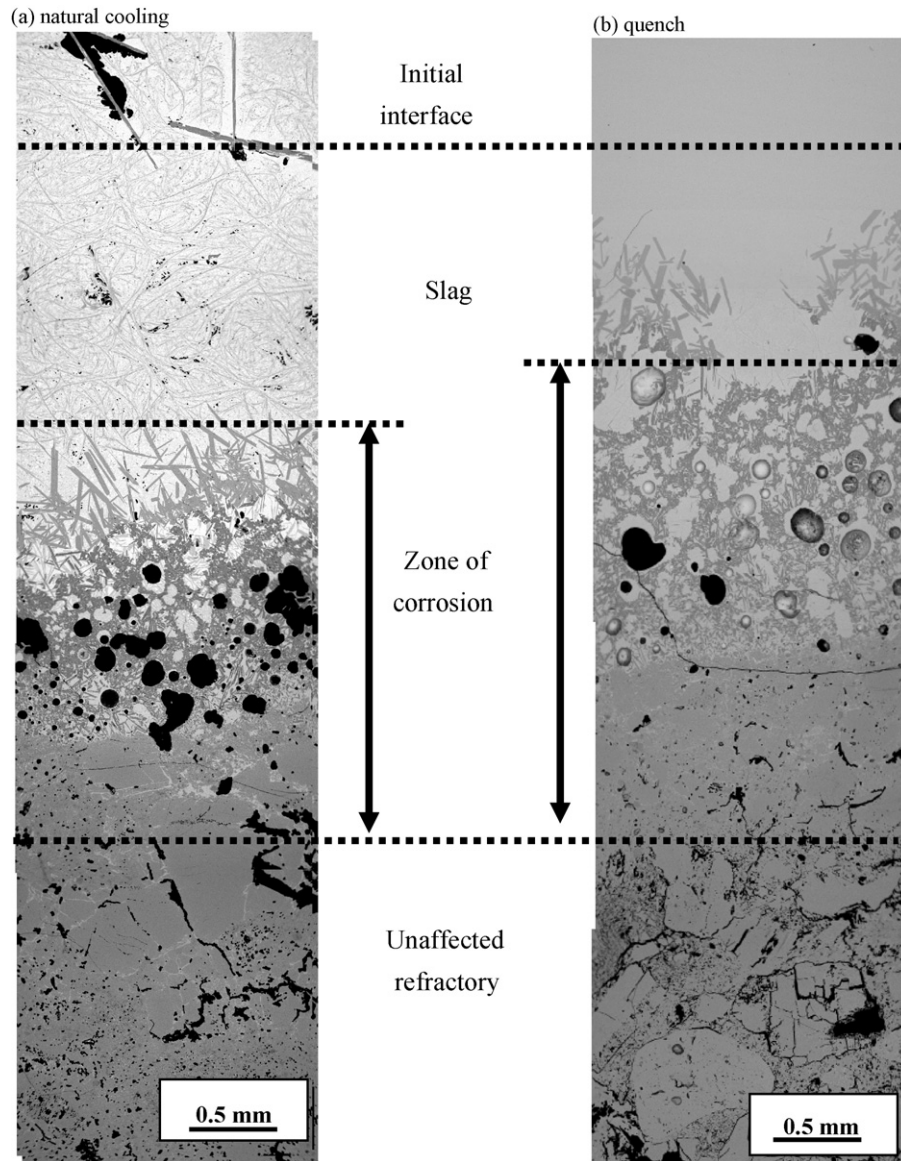


Fig. 1. SEM micrographs of andalusite based refractory in (a) naturally cooled and (b) quenched crucibles (laboratory test:  $T = 1600\text{ }^{\circ}\text{C}$ , 50 wt%  $\text{Al}_2\text{O}_3$ –50 wt% CaO slag and crucible method).

composition of glasses, the evolution of the viscosity of the liquids.

## 2. Experimental procedure and examination of microstructures

Two high alumina refractory materials based on andalusite and bauxite have been selected for the purpose of this research. Their formulations and principal characteristics are indicated in Tables 1 and 2. The typical microstructures of the original bricks are shown in Figs. 2 and 3. For the andalusite refractory, a fine matrix composed of mullite needles in a silica-rich glass binds the coarse grains of mullitized andalusite converted into a mullite/glass composite.<sup>2</sup> The binding glass has a composition similar to that resulting from the mullitization of andalusite ( $\approx 70\%$   $\text{SiO}_2$ ,  $\approx 25\%$   $\text{Al}_2\text{O}_3$ ,  $\approx 2\%$   $\text{Fe}_2\text{O}_3$ ,  $\approx 1\%$   $\text{TiO}_2$  and  $\approx 1\%$   $\text{K}_2\text{O}$ ).

Table 1  
Formulations of andalusite and bauxite bricks (manufacturer data)

Raw material	Size (mm)	Andalusite brick (wt%)	Bauxite brick (wt%)
Randalusite	1–4	30	
Kerphalite KA	0.3–1.6	35	
Kerphalite KF	0–0.16	12	
Kerphalite KF	0–0.055	5	
Chinese bauxite	1–4		32
Chinese bauxite	0–1		33
Chinese bauxite	0–0.16		9
Calcined alumina		14	14
Clay RR40		4	9
Plastifier			3
Total		100	100

Table 2  
Chemical composition, density and apparent porosity of andalusite and bauxite bricks

Refractories	Composition (wt%)								Mineral phases	Density (g/cm <sup>3</sup> )	Apparent porosity (%)
	Al <sub>2</sub> O <sub>3</sub>	SiO <sub>2</sub>	CaO	MgO	Fe <sub>2</sub> O <sub>3</sub>	TiO <sub>2</sub>	Na <sub>2</sub> O	K <sub>2</sub> O			
Andalusite brick	64.1	33.4	0.1	0.1	0.7	0.2	0.1	0.2	M <sup>***</sup> , A <sup>*</sup>	2.65	11.09
Bauxite brick	78.6	11.2	0.4	0.4	1.7	3.3	0.2	0.3	A <sup>***</sup> , M <sup>**</sup> , TiO <sub>2</sub> <sup>*</sup> , (Al, Fe) <sub>2</sub> TiO <sub>5</sub> <sup>*</sup>	3.24	16.17

Mineral phases: A → corundum, M → mullite (\*\*\*: major; \*\*: mean; \*: minor).

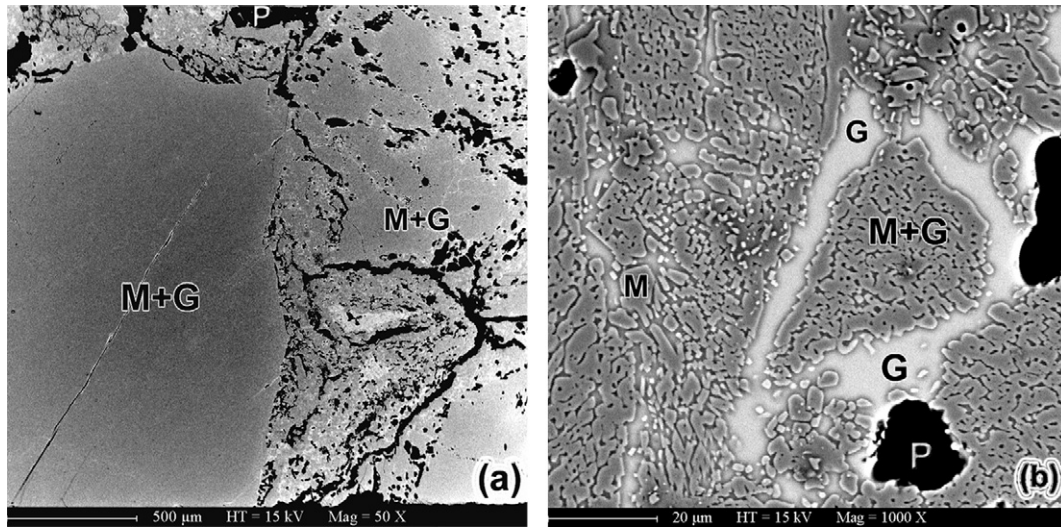


Fig. 2. Backscattered electron images of the typical microstructure of andalusite brick showing the mullite–glass composite and the bonding matrix made from silica-rich glass: (a) low magnification (50×) and (b) high magnification (1000×). M: mullite, G: glass and P: pore.

For the bauxite refractory, coarse grains are composed of corundum with some tialite (titanium aluminate containing some iron). The fine matrix contains corundum, mullite and a glassy phase. The intergranular glass is very fine and has a complex chemical composition ( $\approx 45\%$  SiO<sub>2</sub>,  $\approx 20\%$  Al<sub>2</sub>O<sub>3</sub>,  $\approx 8\%$  Fe<sub>2</sub>O<sub>3</sub>,  $\approx 8\%$  P<sub>2</sub>O<sub>5</sub>,  $\approx 8\%$  TiO<sub>2</sub>,  $\approx 5\%$  CaO,  $\approx 2\%$  MgO,  $\approx 2\%$  K<sub>2</sub>O,  $\approx 1\%$  Na<sub>2</sub>O).

Corrosion tests, using the static crucible method, have been carried out at 1600 °C, in an electric furnace, incorporating an elevating hearth, allowing for the loading and unloading of the crucible. Crucibles of 100 mm × 100 mm × 60 mm in size were cut-out from the bricks, previously fired at 1550 °C for 12 h. After 6 h of corrosion tests, the crucibles were rapidly quenched in water in order to avoid partial crystallization of the liquid phase during cooling.

These laboratory tests were performed with an Al<sub>2</sub>O<sub>3</sub>(50 wt%)-CaO(50 wt%) slag (labelled AC) which is close to that of a ladle slag allowing production of Al killed carbon steels. This synthetic slag was prepared by mixing, in appropriate proportions, powders comprising calcium carbonate (CaCO<sub>3</sub> > 98%, Alfa Aesar) and reactive alumina (CT300SG, Al<sub>2</sub>O<sub>3</sub> > 99.8%).

The post-mortem analysis of the crucibles after testing (Figs. 4 and 5) permitted the identification of four zones<sup>3</sup>:

- the slag zone,
- the precipitation zone,

- the penetration zone,
- the unaffected refractory zone.

### 2.1. The slag zone

After cooling, a glassy slag layer is observed at the bottom of the crucible. Its composition changes with a decrease in CaO and an enrichment in SiO<sub>2</sub>. The Al<sub>2</sub>O<sub>3</sub> content remains nearly constant with andalusite bricks and shows a small increase in the case of bauxite bricks.

### 2.2. The precipitation zone

The precipitation zone is formed by a succession of monomineral layers of crystals surrounded by glass. The glass content may be high and is locally variable (30–80%).

The same mineral succession can be observed in bauxite and in andalusite bricks. From the penetrated zone to the slag zone, three successive monomineral layers are observed:

- corundum Al<sub>2</sub>O<sub>3</sub>,
- calcium hexaaluminate CaAl<sub>12</sub>O<sub>19</sub> (CA<sub>6</sub>),
- calcium dialuminate CaAl<sub>4</sub>O<sub>7</sub> (CA<sub>2</sub>).

The texture and the shape of the layers clearly indicates that the crystals were precipitated slowly from a liquid<sup>4,5</sup> (they do not result from a crystallization during cooling). Corundum from

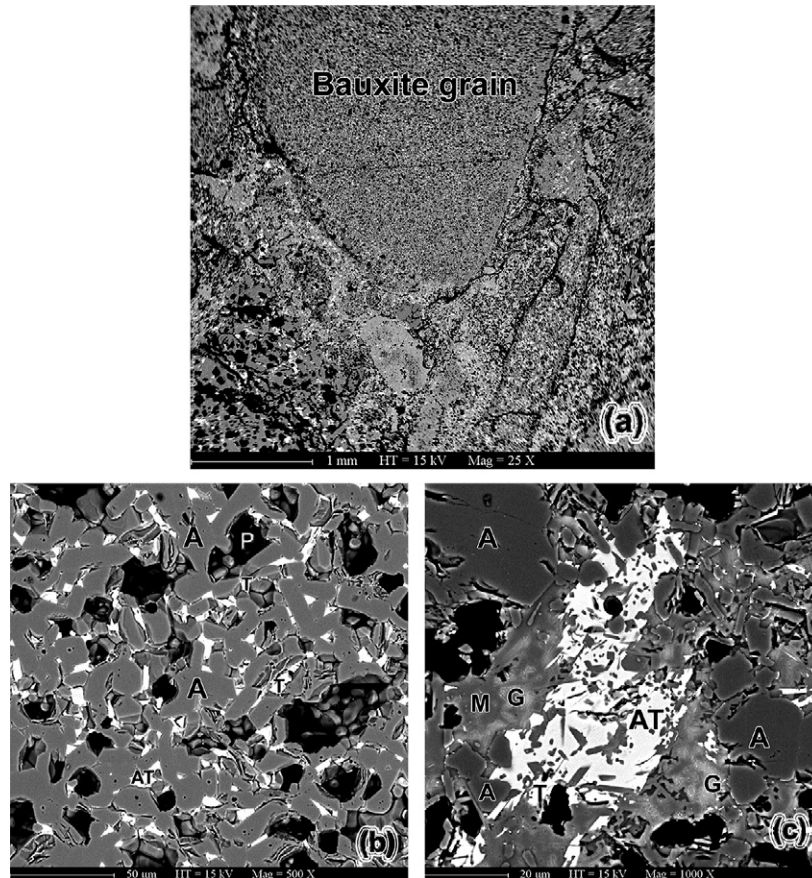


Fig. 3. Backscattered electron images of the typical microstructure of the bauxite brick showing the porous nature of bauxite and a bond matrix made from a mix of corundum (A), mullite (M), aluminum titanate (AT), titania (T) and glass (G): (a) low magnification (25 $\times$ ) and (b): high magnification (500 $\times$ )  $\rightarrow$  microstructures of a grain of bauxite transformed into corundum, (c) high magnification (1000 $\times$ )  $\rightarrow$  the bonding matrix (c); 1000 $\times$ ). AT:  $(\text{Al,Fe})_2\text{TiO}_5$ , T:  $\text{TiO}_2$  and P: pore.

the first layer shows well-formed crystals that differ clearly from those of the transformed bauxite. The  $\text{CA}_6$  phases are still present, but in the case of an important corrosion of the refractory, the  $\text{CA}_2$  phases are absent.

### 2.3. The penetration zone

The viscous slag invades the matrix by capillary penetration and mixes with the pre-existing intergranular liquid by diffusion. The penetration of the corrosive liquid phases leads to the superficial dissolution of the aggregates, so changes affect mainly the matrix with a progressive increase in the glass phase. For the andalusite brick, the limit between the penetrated zone and the precipitation zone is more regular than for the bauxite brick. At that zone limit, dissolution of mullitized andalusite grains seems to be completed by the corrosive liquid, but large bauxite grains converted to corundum may remain beyond in the precipitation zone.

### 2.4. The refractory zone

This zone is composed of unaffected bauxite or andalusite refractories

## 3. Interpretation of corroded microstructures

### 3.1. Equilibrium aspect

In the zone of corrosion, the heterogeneous system refractory/slag is open and exchanges matter with the surrounding. The concept of thermodynamic equilibrium applies to a closed system which exchanges only heat and energy. It requires the chemical potential of each component in all phases to be equal.

When a system is open, equilibrium is not total, but it can be applied on the local scale. The concept of “local equilibrium” is well established in the literature<sup>6,7</sup> and is a fundamental assumption in models of diffusion-controlled reaction.

In a solid–liquid refractory system, chemical exchanges occur through the liquid phase (diffusion, infiltration and percolation). When solid–liquid reactions (dissolution, precipitation) are faster than chemical transport, equilibrium motion may be locally applied:

- the solid phases are locally in equilibrium with the liquid which surrounds them;
- the Gibbs’ phase rule may be used;

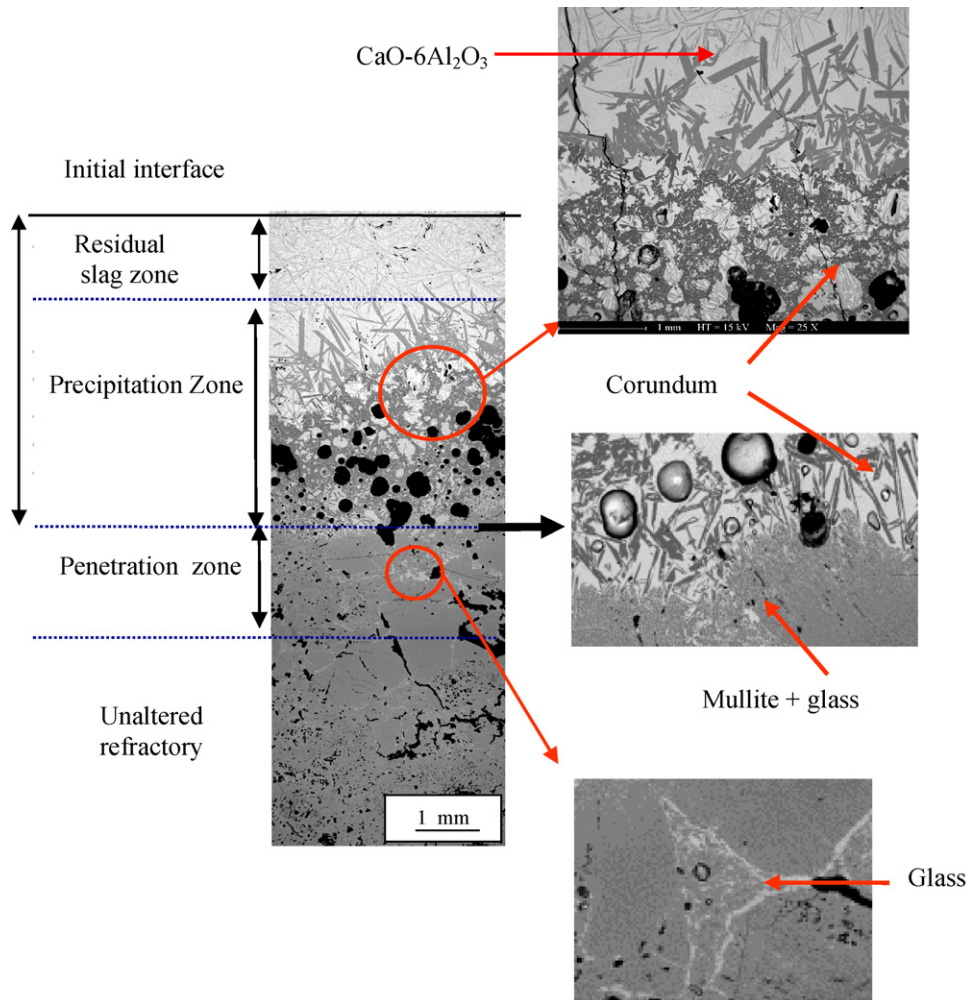


Fig. 4. Microstructure of corroded andalusite refractory by  $\text{Al}_2\text{O}_3$ – $\text{CaO}$  slag attack.

- the chemical mobility entails concentration gradients, which are the driving force of corrosion and will tend to bring the system back towards global equilibrium.

Depending on its local composition, the liquid dissolves the solid phases which are not in equilibrium with it and precipitates new phases after it becomes saturated.

### 3.2. Use of the phase rule

The degree of freedom  $F$  (variance) of the system is given by the phase rule of Willard Gibbs.<sup>8</sup> The following equation gives the usual mathematical form of the phase rule:

$$F = C + 2 - P \quad (1)$$

$C$ : number of components of the system;  $P$ : number of phases present at equilibrium; 2: number of environmental factors (temperature and pressure).

When the temperature and the pressure are fixed, the Gibbs' phase rule reduces to the following equation:

$$F = C - P \quad (2)$$

The phase rule applies only to equilibrium states of a system, which require both homogeneous equilibrium within each phase and heterogeneous equilibrium between co-existing phases. The phase rule does not depend on the nature and amounts of the phases present, but only on their numbers; nor does it give information concerning rates of reactions. Non-conformity with the phase rule is the proof that equilibrium conditions do not exist.

Data from microstructural examinations, described above, have showed that a succession of zones is observed: the initial refractory, the penetration zone, the precipitation zone and the remnant slag. Furthermore, the precipitation zone may contain one or several mono mineral layers.

Consider as an example the corrosion of a 3:2 mullitized andalusite-based refractory by an  $\text{Al}_2\text{O}_3(50 \text{ wt}\%)$ – $\text{CaO}(50 \text{ wt}\%)$  model slag, at 1600 °C.

#### 3.2.1. The initial refractory

The initial refractory is composed of a solid phase ( $3\text{Al}_2\text{O}_3$ – $2\text{SiO}_2$ ) and a liquid phase (a silica-rich glass) which is saturated with mullite ( $P=2$ ). It contains only  $\text{Al}_2\text{O}_3$  and  $\text{SiO}_2$  ( $C=2$ ). The degree of freedom  $F$  (variance) is equal to 0.

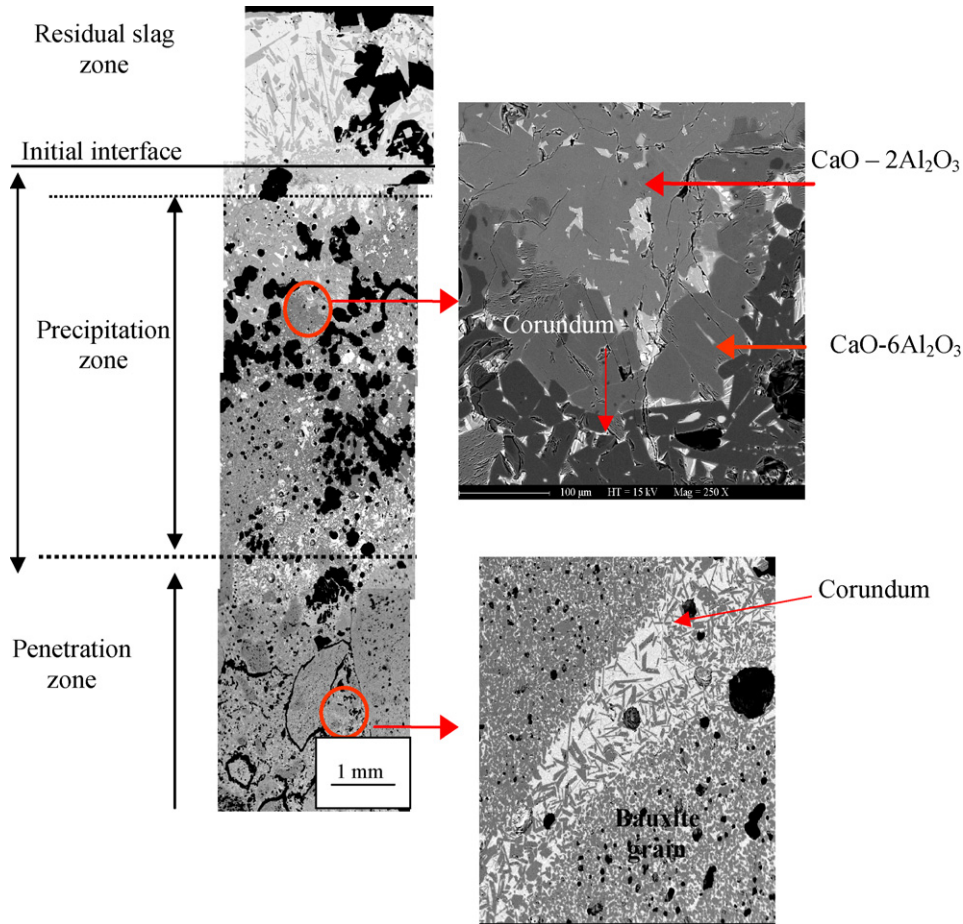


Fig. 5. Microstructure of corroded bauxite refractory by  $\text{Al}_2\text{O}_3$ -CaO slag attack.

Consequently, the composition of the liquid phase is constant and is given by the saturation solubility of the mullite in the liquid phase.

### 3.2.2. The penetration zone

The refractory is partially permeated by the slag. When the lime diffuses through the interstitial liquid, the number of components  $C$  increases to 3 whereas the number of phases  $P$  remains equal to 2. The degree of freedom becomes equal to 1, and the composition of the liquid is not constant any more. The concentrations of alumina, lime and silica vary in the liquid.

### 3.2.3. The precipitation zone

In this zone, located between the slag and the zone of impregnation, newly crystalline phases precipitate during the reactions refractory/slag. The liquid contains three oxides  $\text{Al}_2\text{O}_3$ , CaO,  $\text{SiO}_2$ ; the number of components  $C$  is equal to 3. The degree of freedom  $F$  can never be less than 0 under invariant conditions. Consequently, the number of phases  $P$  cannot exceed 3: two solids and one liquid. When two solid phases coexist, the variance is equal to 0 and the composition of the liquid is constant. However, because of diffusion and of the chemical gradients, the concentration of an element in the liquid varies regularly depending on the distance and the time period. At the end of a time  $t$ , the conditions of equilibrium between two solid phases

can exist only at a given distance from the initial interface. Lastly, when only one solid phase is present, the variance is equal to 1, and the composition of the liquid can vary.

The new phases which crystalline during dissolution-precipitation processes<sup>9</sup> consist of different successive monomineral layers separated by sharp boundaries.

### 3.3. Prediction of reaction products at refractory/slag interface

At the initial stage of the reaction, on both sides of the initial interface, there is liquid slag (50% CaO and 50%  $\text{Al}_2\text{O}_3$ ) and a siliceous liquid which impregnate the mullite aggregates of the andalusite-based refractory. This initial situation is described in Fig. 6. For more simplicity, consider the example of a slag containing the element A and a refractory containing the element B. The slag and the refractory are coupled according to a plane initial interface.

In the slag, all are liquid, the concentration of element A is high ( $C_{\text{Slag}}^A$ ), and that of the element B is equal to 0. In the refractory, composed of the phase B, there is a little liquid with a high concentration of B ( $C_B^B = \text{solubility of B in the liquid}$ ), while the concentration of A is equal to 0.

On both sides of the initial interface, there is a “step” of chemical concentration. This situation is unstable, and the step

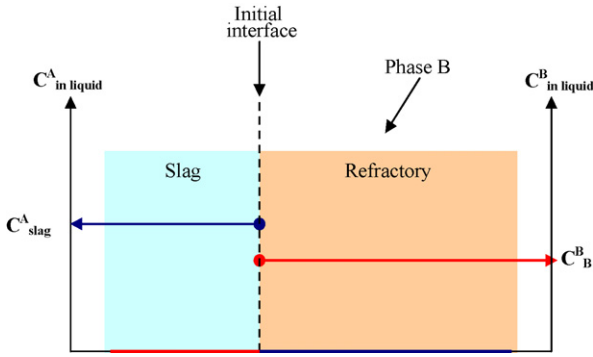


Fig. 6. Initial stage of corrosion between a refractory and a liquid slag.

will be transformed into a gradient of concentration: element A of the slag will migrate towards the liquid of the refractory, and element B of the refractory will migrate towards the slag. Fig. 7 shows the evolution of the reaction.

Consider that, in the system A–B, exist the different phases A, AB, AB<sub>2</sub>, and B. The concentrations at equilibrium, in the liquid, are as follows:

- solubility of the phase B in the liquid slag:  $C_B^B$
- concentrations, respectively of A and B in the liquid phase in equilibrium with the assembly B + AB<sub>2</sub>:  $C_{AB_2/B}^A$  and  $C_{AB_2/B}^B$
- concentrations, respectively of A and B in the liquid phase in equilibrium with the assembly AB<sub>2</sub> + AB:  $C_{AB/AB_2}^A$  and  $C_{AB/AB_2}^B$ .

As long as the concentration of A in the liquid remains lower than  $C_{AB_2/B}^A$  (in equilibrium with the phases A + B), it will be localized in the zone of infiltration. The increase in the concentration of A in the liquid and the decrease in B which diffuses towards the slag, involves a dissolution of phase B.

When the concentration in A exceeds  $C_{AB_2/B}^A$ , the phase AB<sub>2</sub> becomes stable and precipitates while phase B disappears by dissolution. Phase AB<sub>2</sub> remains the only stable solid phase as long as the concentration of A in the liquid remains lower than  $C_{AB/AB_2}^A$ .

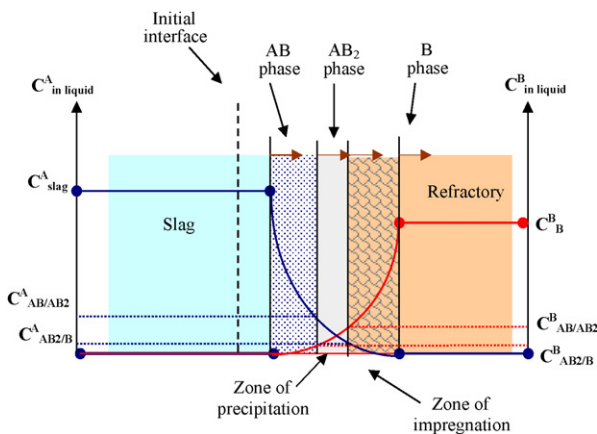


Fig. 7. Evolution of the corrosion of a solid refractory by liquid slag. Formation of a zone of impregnation, reactional monomineral zones and displacement of the interfaces.

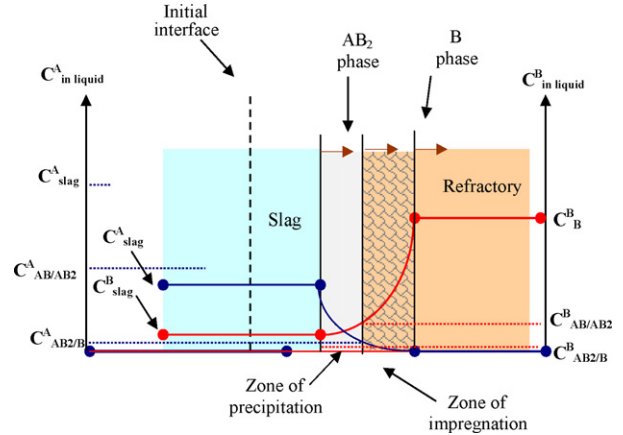


Fig. 8. Evolution of the corrosion of a solid refractory by liquid slag. Disappearance of the monomineral zone of AB when the concentration of A is decreasing in the slag.

Thus, there is the formation of a monomineral zone of AB<sub>2</sub>. Beyond this limit, the phase AB precipitates and forms a second monomineral zone. The latter is gradually dissolved in the slag.

Various monomineral zones separated by boundaries are obtained which move gradually while advancing on refractory material.

Theoretically, in a semi-infinite system, the number of monomineral zones which are formed is equal to the number of intermediate compounds likely to be formed between the phases A and B. In practice, in the laboratory tests, the quantity of slag is limited and its composition changes. The migration of calcium towards refractory involves a decrease in the concentration of this element in the slag which can be lower than the concentration  $C_{AB/AB_2}^B$  in equilibrium with the assembly AB + AB<sub>2</sub>. Phase AB is not stable any more, and the corresponding monomineral zone disappears as Fig. 8 shows.

The Al<sub>2</sub>O<sub>3</sub>–CaO–SiO<sub>2</sub> phase diagram<sup>9</sup> makes it possible to determine which are the phases likely to appear during the corrosion of high alumina by Al<sub>2</sub>O<sub>3</sub>–CaO. It also makes it possible to predict the succession of the reactional zonations for each kind of refractories:

- mullitized andalusite-based refractory: slag/dialuminate of calcium/hexaaluminate of calcium/corundum/mullite
- bauxite-based refractory: slag/dialuminate of calcium/hexaaluminate of calcium/corundum
- alumina-based refractory: slag/dialuminate of calcium/hexaaluminate of calcium/corundum

For example, Figs. 9 and 10 show microstructures of the precipitation zones of bauxite and andalusite refractories after corrosion. The alteration of the refractory microstructures can be explained by dissolution–precipitation processes inside a liquid phase.<sup>5</sup> Several mineral layers can be observed.

The same succession will be observed for all the types of slag as long as their initial composition does not differ too much from a ratio C/A + S close to 1. This zonation corresponds to the maximum number of observable monomineral zones, knowing that

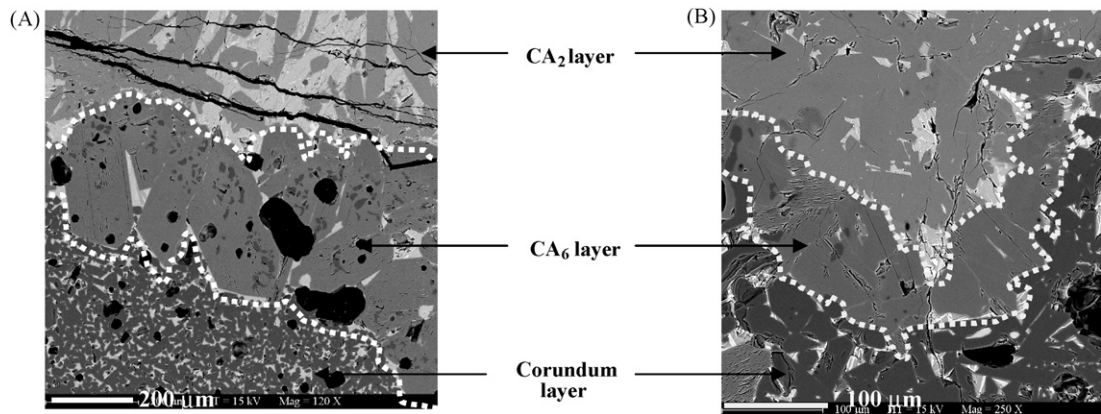


Fig. 9. Corrosion of bauxite brick by  $\text{Al}_2\text{O}_3\text{--CaO}$  slag; backscattered electrons SEM micrographs. (A) Transition between the three monomineral layers of the precipitation zone and (B) neogenic layer made of large well-formed corundum crystals developed at the expense of small badly formed corundum issued from the transformation of a bauxite grain. C: corundum;  $\text{CA}_2$ : calcium dialuminate;  $\text{CA}_6$ : calcium hexaaluminate. The light-grey background represents the high-temperature liquid phase partially recrystallized during cooling.

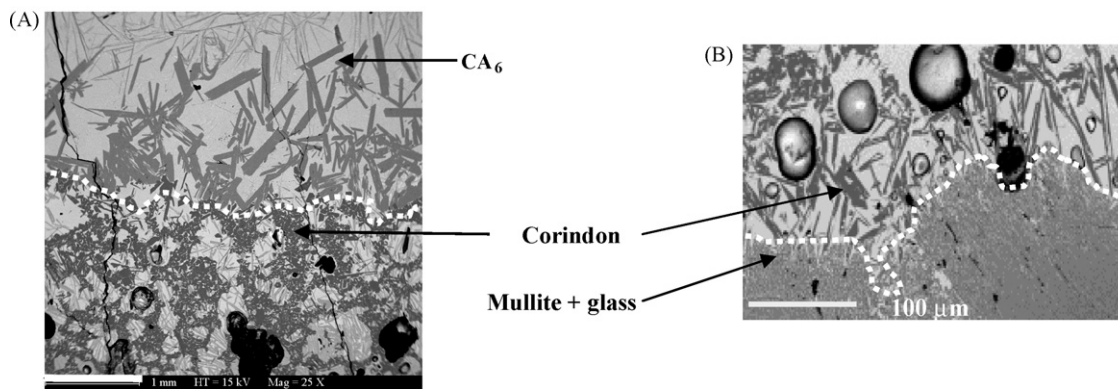


Fig. 10. Corrosion of andalusite brick by  $\text{Al}_2\text{O}_3\text{--CaO}$  slag; backscattered electrons SEM micrographs. (A) Transition between the calcium hexaaluminate ( $\text{CA}_6$ ) and the corundum layers and (B) transition between the corundum layer of the precipitation zone and the refractory (mullite + glass) C: corundum;  $\text{CA}_2$ : calcium dialuminate;  $\text{CA}_6$ : calcium hexaaluminate; M: mullite. The light-grey background with the needle-like crystals localized in the corundum layer in (A) represents the high-temperature liquid phase partially recrystallized during cooling and converted to anorthite ( $\text{CAS}_2$ ) and residual glass.

the evolution of the composition of the slag during the reaction can make the most external zones to disappear.

#### 4. Determination of the composition profiles of the liquid phase at high temperature

##### 4.1. Method

The gradients of concentration, which exist in the liquid phase at high temperature are the driving force behind corrosion processes at high temperature. Unfortunately, two phenomena make it difficult to determine the composition of this liquid.

- On the one hand, the partial crystallization of the liquid during cooling does not make it possible to assimilate the composition of residual glass (which can be determined by EDS analysis) with that of the liquid which existed at high temperature. The only representative analysis would be an EDS mapping of a zone including residual glass and the crystals formed during cooling.

- In addition, the existence of monomineral zones with newly formed solid phases in the liquid make the analyses by mapping non-representative, since, they integrate not only the crystals formed during cooling and residual glass, but also the crystals newly formed.

One of the possibilities consists in carrying out a fast quench at the end of the corrosion test to limit the crystallization of the liquid during cooling. Under these conditions, the only crystallized phases are due to corrosion and the microanalyses of glass between the crystals are representative of glass at high temperature.

Concurrently with this direct method, an indirect method can be implemented. It consists in using the analyses (obtained by mapping) which are carried out on the totality of the corroded zone. The results are interpreted using the phases diagrams and the concept of “local equilibrium”.

Fig. 11 shows the principle of the method. Within the framework of the “local equilibrium concept”, the information which is provided by the phase diagrams is limited:



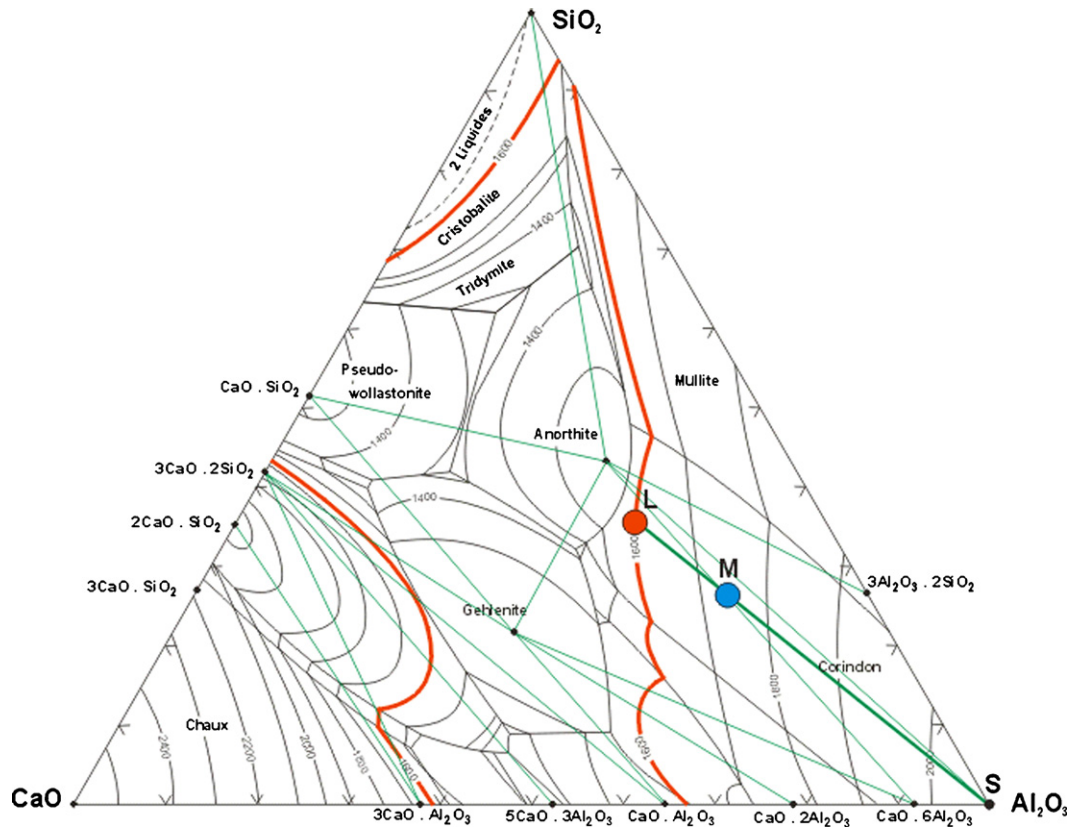


Fig. 11. Determination of the composition of the liquid at 1600 °C for an analysed zone represented by point M (thick line: 1600 °C isotherm line).

- the point L is representative of the composition of the liquid at 1600 °C;
- the composition represented by the point M corresponds to an assemblage of a liquid and a solid phase at 1600 °C.

The diagram  $\text{Al}_2\text{O}_3\text{--CaO--SiO}_2$  gives no direct information on the composition, neither of the liquid, nor of the solid corresponding to the point M. It cannot be used like a diagram of thermodynamic equilibrium. However, its use as a ternary diagram of composition remains valid. A surface analysed by mapping with the scanning electron microscopy (SEM) consists of liquid and newly formed solids during corrosion at 1600 °C. Those can be distinguished from the phases formed by the crystallization of glass during cooling.

For an analysed zone, represented by the point M, in which the solid phase is the corundum (point S), the liquid at 1600 °C is represented by the point L obtained by the intersection of the segment SM with the isotherm 1600 °C of the diagram. The proportion of liquid is given by the ratio  $\text{MS}/\text{LS}$ , and the composition of this liquid is deduced from the position of the point L in the triangle of composition.

In a certain number of cases, the analysed surface is situated on several zones of reaction and contains several phases: for example, mullite + corundum, or corundum + CaO. In strictly speaking, it would be necessary to consider the relative proportion of the two phases and to place the point representative of the solid in proportion on the segment which joins these two solids.

#### 4.2. Validation of the method and results

Composition profiles (chemistry as a function of distance from the initial interface), established for the mullitized andalusite based refractory in contact with a  $\text{Al}_2\text{O}_3\text{--CaO}$  slag, by the direct method (quench of the liquid phase at the end of the corrosion test) and the indirect method (concept of local equilibrium applied to phase diagram) are given in Fig. 12. The data obtained by these two methods are in agreement.

Across the modified area (zone II and III), the liquid composition presents gradients of concentration connecting the composition of the interstitial liquid in the refractory to the slag.

The chemical exchanges occur through the liquid phase. Depending on its local composition, the liquid dissolves the solid phases which are not in equilibrium with it and precipitates new phases after it becomes saturated.<sup>10</sup>

Fig. 13 shows an other compositional profile of the liquid phase associated with the zonation of mineral solid phases present at a temperature of 1600 °C (mullitized andalusite refractory,  $\text{Al}_2\text{O}_3\text{--CaO}$  slag and quench).

For each zone, the equilibrium constants, the number of phases in equilibrium and the variance of the system are determined.

##### 4.2.1. Zone of the initial refractory

At this depth, CaO does not infiltrate. The liquid is composed of  $\text{Al}_2\text{O}_3$  and  $\text{SiO}_2$ . As  $[\text{Al}_2\text{O}_3] + [\text{SiO}_2] = 1$ , alumina and

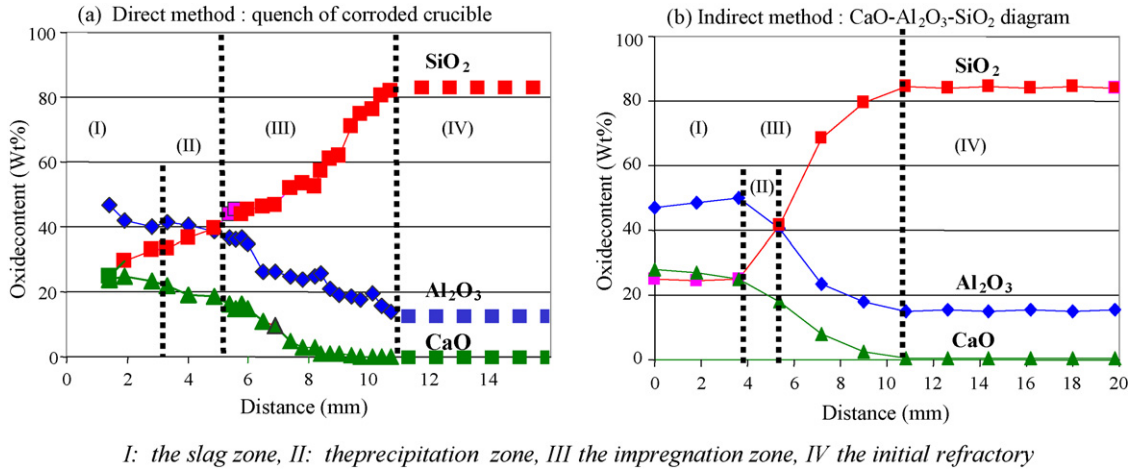
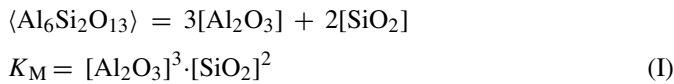


Fig. 12. Compositional profile of the intergranular-liquid phase in the andalusite refractory (a: experimental values, b: obtained with the Al<sub>2</sub>O<sub>3</sub>–CaO–SiO<sub>2</sub> phase diagram).

silica contents are fixed. The liquid is saturated with mullite, the saturation is defined by the equilibrium constant  $K_M$  of the reaction:



$\langle \cdot \rangle$  means “in the solid state” and  $[\cdot]$  “dissolved in a liquid phase”

The liquid composition is then constant and the degree of freedom is 0.

4.2.2. Impregnation zone

CaO infiltrates the interstitial liquid. As a consequence, the liquid composition will not be in equilibrium with mullite, which

gradually dissolves until it totally disappears at the boundary separating the zones of penetration and precipitation. The composition of the liquid phase is not constant any more and the degree of freedom becomes equal to 1.

4.2.3. Boundary between the impregnation zone and the precipitation zone

Two mineral phases coexist: residual mullite and neofomed corundum. The liquid phase is simultaneously in equilibrium with corundum and mullite (C/M equilibrium). The corundum saturation is expressed by the reaction constant:



Al<sub>2</sub>O<sub>3</sub> and SiO<sub>2</sub> contents are both constant:

$$[\text{Al}_2\text{O}_3]_{C/M} = K_C \text{ and } [\text{SiO}_2]_{C/M} = K_C^{-1} \left( \frac{K_M}{K_C} \right)^{1/2}$$

As the liquid contains only three species, the concentration of CaO can be determined by means of the following equation:

$$[\text{CaO}]_{C/M} = 1 - ([\text{Al}_2\text{O}_3]_{C/M} + [\text{SiO}_2]_{C/M})$$

It thus appears clearly that the contents of the three constituents of the liquid are fixed at the boundary between the zones of precipitation and penetration.

The degree of freedom is equal to 0.

This result is consistent with data obtained from composition profiles previously established (either by direct analysis of glass or using a CaO–Al<sub>2</sub>O<sub>3</sub>–SiO<sub>2</sub> diagram) which revealed the existence of a constant composition at this interface whatever the nature of the slag. In the precipitation zone, a first monomineral layer containing corundum formed during corrosion at 1600 °C is observed. Equilibrium of liquid with corundum is defined by reaction (II) mentioned above. It follows that Al<sub>2</sub>O<sub>3</sub> content is fixed in this zone ( $[\text{Al}_2\text{O}_3]_C = K_C$ ), and concentrations of CaO and SiO<sub>2</sub> must inversely vary because their sum has to remain constant. It must be noted that corundum is really stable only near the surface of the refractory where it precipitates, while

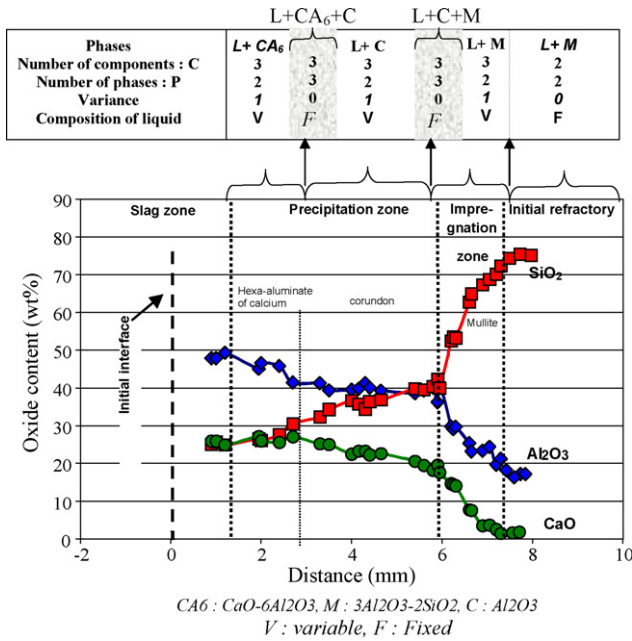


Fig. 13. Another compositional profile of the liquid phase associated with the zonation of the mineral solid phases present at 1600 °C (mullitized andalusite refractory, Al<sub>2</sub>O<sub>3</sub>–CaO slag, quench).

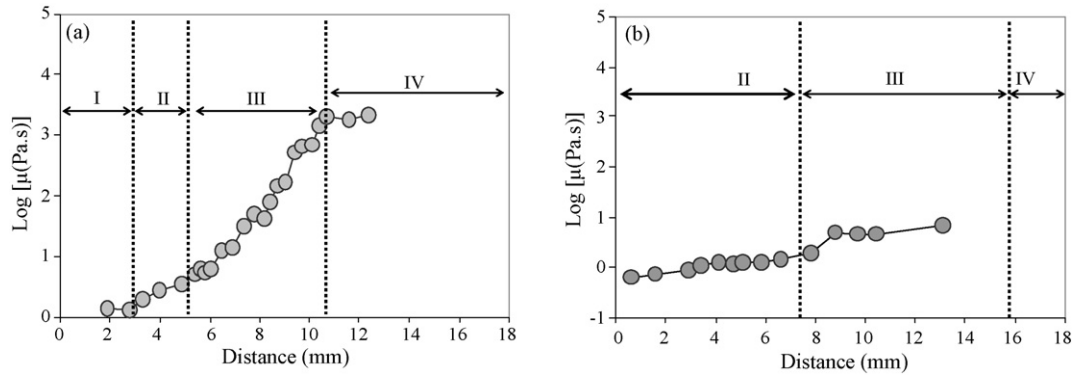


Fig. 14. Viscosity profiles of the liquid phase in the tested andalusite (a) and bauxite (b) refractories, according to Urbain's model. (I) slag zone, (II) precipitation zone, (III) penetration zone, and (IV) unaffected refractory. Initial slag–refractory interface is located at  $d=0$  mm. Note that zone IV in (b) is less wide than in (a) because of deep penetration of slag in brick B.

far from the corrosion front, it dissolves to maintain a constant  $\text{Al}_2\text{O}_3$  content in the liquid and thus to make up for the increase in the CaO content.

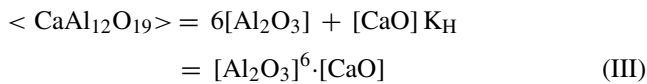
#### 4.2.4. Precipitation zone

- Monomineral layer of corundum

Along the  $\text{CA}_6$  layer, concentrations of  $\text{Al}_2\text{O}_3$ , CaO and  $\text{SiO}_2$  are variable. The degree of freedom is equal to 1.

- Boundary between the corundum and the hexaaluminate of calcium layers

At the interface between layers of corundum and  $\text{CA}_6$ , the liquid is saturated with these two phases, thus corresponding to equilibrium between reaction (II) and (III):



The concentrations of CaO and  $\text{Al}_2\text{O}_3$  are defined as follows at this interface:

$$[\text{Al}_2\text{O}_3]_{\text{C/H}} = K_C \quad \text{and} \quad [\text{CaO}]_{\text{C/H}} = \frac{K_H}{K_C^6}$$

As  $[\text{Al}_2\text{O}_3] + [\text{CaO}] + [\text{SiO}_2] = 1$ , the  $\text{SiO}_2$  concentration is also determined at the interface. The degree of freedom is equal to 0.

- Monomineral layer of hexaaluminate of calcium

Along the  $\text{CA}_6$  layer, concentrations of  $\text{Al}_2\text{O}_3$ , CaO and  $\text{SiO}_2$  are variable. The degree of freedom becomes equal to 1.

- Boundary between the precipitation zone and the slag zone

$\text{CA}_6$  disappears at the boundary interface. Beyond this interface, there is no more liquid phase.

#### 4.3. Viscosity of the liquid phases

The gradient of the chemical composition of the intergranular liquid phase plays a fundamental role. The viscosity of the liquid phase is the second parameter, which influences the migration of the species in this liquid.

Viscosity  $\eta$  was calculated according to Urbain's model<sup>11</sup> by the following equation:  $A\text{Tex}p(10^3 B/T)$ , A and B are two parameters depending on the composition of the glass. The viscosity of the intergranular liquid phase is shown in Fig. 14 for (a) and (b) andalusite and bauxite refractories.

EDS analysis of the glass in the two refractories integrates all the elements of the slag–refractory system including the impurities. For bauxite refractory, in which there is no residual slag zone (absence of zone I corresponding to the part of refractory replaced by slag), a low viscosity of the liquid phase, due to the presence in a high content of minor elements (amounting ~20–30%) such as  $\text{Fe}_2\text{O}_3$ ,  $\text{P}_2\text{O}_5$ ,  $\text{TiO}_2$ , alkaline and earth–alkaline oxides, is observed along the modified part of the refractory (area extending from the unaffected zone to the slag zone). This fact explains why the penetration zone is wider in bauxite than in andalusite refractory. Furthermore, the fraction of impurities coming from raw materials may be negligible in the andalusite brick, so that the liquid phase is considered to be predominantly  $\text{CaO} + \text{Al}_2\text{O}_3 + \text{SiO}_2$ .

For andalusite refractory, the liquid viscosity is constant along the slag zone (zone I;  $\mu \approx 1$  Pa s) as well as in the unaffected refractory (zone IV;  $\mu \approx 1570$  Pa s). From the unaffected zone, a considerable decrease in the liquid viscosity is observed up to the precipitation zone. The liquid becomes more fluid near the corrosion front and easily infiltrates the grain boundaries leading to the dissolution of most present fine phases. As a result, the dissolved phases become part of the local liquid, thus increasing the liquid content. However, an explanation for the lack of deep slag penetration in andalusite refractory lies in the fact that a high amount of viscous liquid (silica-rich with a lower content of secondary oxides) is formed in the part of the refractory in contact with the slag, which slowed down the penetration of the slag.

## 5. Conclusion

The corrosion mechanisms of refractories by liquid oxides are far from being completely known. The study of microstructures, which improves our knowledge of corrosion, is extremely useful to determine the mechanisms of chemical attack. However,

the microstructures of corroded refractories are very difficult to interpret.

In this paper, an approach based on the concept of local thermodynamic equilibrium and the use of the phase rule is proposed to analyse the microstructures.

An experimental corrosion study of high-alumina refractories by an alumina–lime model slag is carried out to illustrate this approach. The post-mortem analysis of microstructures after testing, revealed the development of a penetration zone, followed by a precipitation zone formed of a succession of monomineral layers and show the existence of composition gradients in the interstitial liquid. The local chemical equilibrium concept makes it possible to explain the observed mineral zonation, and to quantify the proportion and composition of the liquid at high temperature from chemical profiles, established by analyzing successive zones by means of scanning electron microscopy.

The composition profiles are compared to those obtained by direct analysis of the interstitial glass in refractories after quenching.

The viscosity profiles, estimated by means of Urbain's model from the composition profiles of the liquid phase, showed that the viscosity of the interstitial liquid determines the extension of the penetration zone in a given refractory.

These results clearly validate this thermodynamic approach which offers new prospects to develop more corrosion-resistant refractories.<sup>12</sup>

## References

1. Lee, W. E., Characterisation of corrosion mechanisms in refractories by post-mortem microstructural analysis. *Br. Ceram. Proc.*, 1997, **57**, 7–15.
2. Ildfonse, J. P., Gabis, V. and Cesbron, F., Mullitization of andalusite in refractory bricks. *Key Eng. Mater.*, 1997, **132–136**, 1798–1801.
3. Qafssaoui, F., Rôle et effet de l'andalusite sur le comportement à la corrosion des céramiques réfractaires à haute teneur en alumine par les laitiers sidérurgiques, PhD Thesis. University of Orleans, France, 2004.
4. Zhang, S., Rezaie, H. R., Sarpoolaky, H. and Lee, W. E., Alumina dissolution into silicate slag. *J. Am. Ceram. Soc.*, 2000, **83**(4), 897–903.
5. Guha, J. P., Reaction chemistry in dissolution of polycrystalline alumina in lime–alumina–silica slag. *Br. Ceram. Trans.*, 1997, **96**(6), 231–236.
6. Thompson Jr., J. B., Local equilibrium in metasomatic processes. In *Researches in Geochemistry, Vol 1*, ed. P. H. Abelson. John Wiley & Sons, New York, 1954.
7. Mueller, R. F., Mobility of elements during metamorphism. *J. Geol.*, 1967, **75**, 565–582.
8. Gibbs, J. W., Equilibrium of heterogeneous substances. *Trans. Conn. Acad. Sci.*, 1874, **3**, 108–248; Gibbs, J. W., Equilibrium of heterogeneous substances. *Trans. Conn. Acad. Sci.*, 1878, **3**, 343–524.
9. Gentile, A. L. and Foster, W. R., *Phase Diagrams for Ceramists*. The American Ceramic Society, Columbus, OH, USA, 1963, p. 220.
10. Qafssaoui, F., Poirier, J., Ildfonse, J. P., Hubert, P. and Benyaich, F., Microstructural and physicochemical studies of corroded high-alumina refractories. *Silicates Ind. Ceram. Sci. Technol.*, 2005, **70**(7–8), 109–117.
11. Urbain, G., Viscosity estimation of slags. *Steel Res.*, 1987, **58**(3), 111–116.
12. Poirier, J., Bouchetou, M. L., Qafssaoui, F. and Hubert, P., Corrosion of high alumina refractories by Al<sub>2</sub>O<sub>3</sub>/CaO slag under thermal cycling conditions. *Interceram. Int. (Part 1 and Part 2)*, 2006, **55**(4), 270–272, and 348–351.